

# Kinetic Modelling of the Influence of H<sub>2</sub>S on Dibenzothiophene Hydrodesulfurization in a Batch System over Nano-MoS<sub>2</sub>

Hamdy Farag<sup>1,2\*</sup>, Abdel-Nasser A. El-Hendawy<sup>3</sup>, Masahiro Kishida<sup>1</sup>

<sup>1</sup>Department of Material Process Engineering, Graduate School of Engineering, Kyushu University, Fukuoka, Japan

<sup>2</sup>Chemistry Department, Faculty of Science, Mansoura University, Mansoura, Egypt

<sup>3</sup>Physical Chemistry Department, National Research Center, Cairo, Egypt

Email: \*faragha@hotmail.com

**How to cite this paper:** Farag, H., El-Hendawy, A.-N.A. and Kishida, M. (2020) Kinetic Modelling of the Influence of H<sub>2</sub>S on Dibenzothiophene Hydrodesulfurization in a Batch System over Nano-MoS<sub>2</sub>. *Advances in Chemical Engineering and Science*, 10, 135-148.

<https://doi.org/10.4236/aces.2020.103010>

**Received:** July 5, 2019

**Accepted:** June 1, 2020

**Published:** June 4, 2020

Copyright © 2020 by author(s) and Scientific Research Publishing Inc. This work is licensed under the Creative Commons Attribution International License (CC BY 4.0).

<http://creativecommons.org/licenses/by/4.0/>



Open Access

## Abstract

In this work, the possibility of enhanced activity during the hydrodesulfurization of dibenzothiophene over certain nano-MoS<sub>2</sub> catalyst due to the presence of H<sub>2</sub>S was examined by focusing on the reaction kinetics. With H<sub>2</sub>S generated *in situ*, the overall reaction followed the autocatalytic rate law; while in the absence of H<sub>2</sub>S the kinetics indicated a pseudo-first-order reaction. H<sub>2</sub>S appears to modify the relative contributions of parallel hydrogenation and desulfurization reactions by drastically increasing the hydrogenation rate. Kinetic models were developed that describe the hydrodesulfurization reaction at various H<sub>2</sub>S concentrations, and the kinetic parameters and adsorption equilibrium constants associated with this process were estimated by fitting the experimental data. The results suggest that the promotion and/or inhibition of hydrodesulfurization by H<sub>2</sub>S likely result from the same overall reaction mechanism.

## Keywords

Hydrodesulfurization, MoS<sub>2</sub>, Kinetics, Model, Autocatalysis, Dibenzothiophene

## 1. Introduction

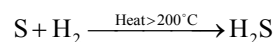
Petroleum is known to be the main source of fuel energy all over the world and will remain so until at least a few decades. As a means of reducing environmental contamination to coincide with the widely adopted legislations for sulfur and nitrogen, it is important to remove sulfur compounds from middle distillate fuels, typically using hydrodesulfurization (HDS). However, polyaromatic sulfur

species constitute the major portion of the sulfur containing compounds in this fuel and are difficult to fully degrade via this catalytic process [1]-[6]. During HDS, the activity of catalysts is affected by the presence of various reaction matrixes, and H<sub>2</sub>S is one that is known to greatly slow down the rate of the reaction by inhibiting the hydrogenolysis of C-S bonds [1] [2]. Nevertheless, under such conditions, the sulfur substrate species must be reacted under the presence of H<sub>2</sub>S. Many studies based on either fixed bed systems or batch reactors have reported drastic suppression of the catalysis of the HDS reaction involving both model sulfur compounds and real feed stocks in the presence of H<sub>2</sub>S [7] [8] [9] [10]. Such behavior is well-known in this area of research where the consensus catalysts are subjected to seriously lose their overall activity because of H<sub>2</sub>S. The extent of activity reduction is varied and highly dependent on the catalyst identity where the established reaction network of sulfur substrate is important. However, interesting results concerning the HDS of dibenzothiophene (DBT) and 4,6-dimethyldibenzothiophene were recently reported [11] [12], which showed that H<sub>2</sub>S may actually promote the HDS activity of some certain MoS<sub>2</sub> class catalysts. To the best of our knowledge, such results are interesting and yet there is surprisingly a lack of literature on following and widely investigating this point. Thus, kinetic modeling that thoroughly describes this approach is needed. The overall catalytic activity and selectivity appear to be dependent on the concentration of H<sub>2</sub>S in the reaction media. Overall, it is evident from the results to date that H<sub>2</sub>S somehow modifies the chemical nature of the active sites in this reaction. To investigate the catalyst activity promotion phenomenon by H<sub>2</sub>S and to determine the adsorption equilibrium constants, the present work performed a number of DBT HDS experiments in conjunction with a MoS<sub>2</sub> catalyst under various conditions, and derived detailed kinetic models to assist in understanding the reaction mechanism.

## 2. Experimental

A model MoS<sub>2</sub> catalyst was prepared by a heat treatment procedure previously described in the literature [11]. Briefly, a precursor of ammonium heptamolybdate tetrahydrate (NH<sub>4</sub>)<sub>6</sub>Mo<sub>7</sub>O<sub>24</sub>·4H<sub>2</sub>O were subjected to a gradual thermal annealing till reaching to 850 °C under a stream of H<sub>2</sub>S/H<sub>2</sub> (10% v/v) gas. After synthesis, the catalyst was milled using zirconia balls and then sulfided at 400 °C and 1 atm under a 10% v/v H<sub>2</sub>S/H<sub>2</sub> gas mixture flowing at 100 sccm in preparation for the experimental trials. All reactions were carried out in a 100 ml batch-type micro-autoclave from which aliquots were withdrawn at specific time intervals, using 100 mg of the catalyst for each trial. The feed consisted of 1 wt% DBT in decane although, in some experiments, 500 mg Cu powder was also added as a H<sub>2</sub>S scavenger to establish the initial kinetics without matrix interference [13]. The use of this type of reactor allowed the effects of the reaction matrix and operating conditions to be examined. All reactions were performed at 340 °C and an initial H<sub>2</sub> pressure of 3 MPa. The H<sub>2</sub>S concentration in the reaction mixture was

changed by adding various quantities of S powder to the autoclave. This S was converted quantitatively to H<sub>2</sub>S by reaction with H<sub>2</sub>, as confirmed by a blank test according to the following equation.



### 3. Results and Discussion

The major products detected following the HDS of DBT were biphenyl (BP), cyclohexylbenzene (CB), partially hydrogenated DBT (HDBT) and H<sub>2</sub>S. As noted, various H<sub>2</sub>S concentrations were employed during the HDS reaction, and **Figure 1** and **Figure 2** summarize the intermediate products obtained from hydrogenation (HYD) and direct desulfurization (DDS) reactions during the HDS of DBT. The formation of these products depended on whether the H<sub>2</sub>S that was generated *in situ* was removed from or retained in the reaction mixture. Specifically, HYD products were generated in greater proportion in the presence of H<sub>2</sub>S, while the DDS products were decreased. It is interesting to note from **Figure 2** the non-linear nature of the HYD route products.

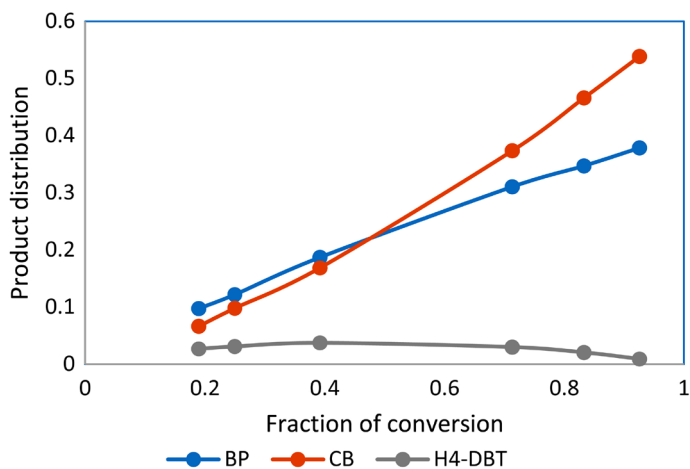


**Figure 1.** Product distributions during the HDS of DBT in the absence of H<sub>2</sub>S.

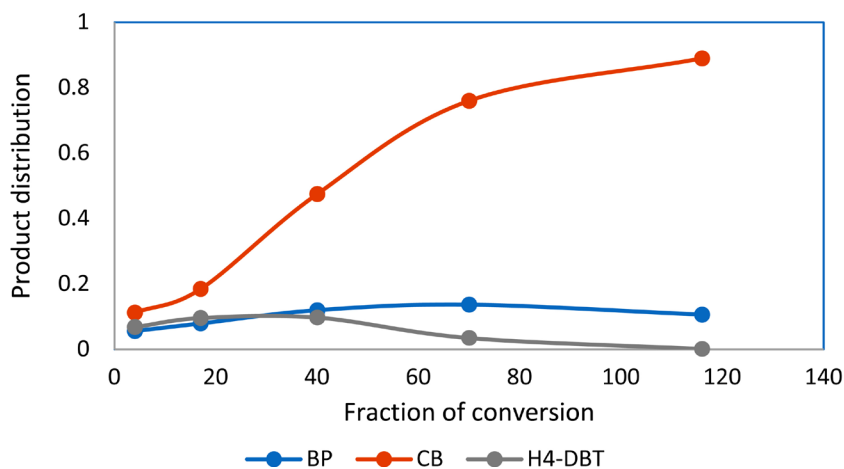
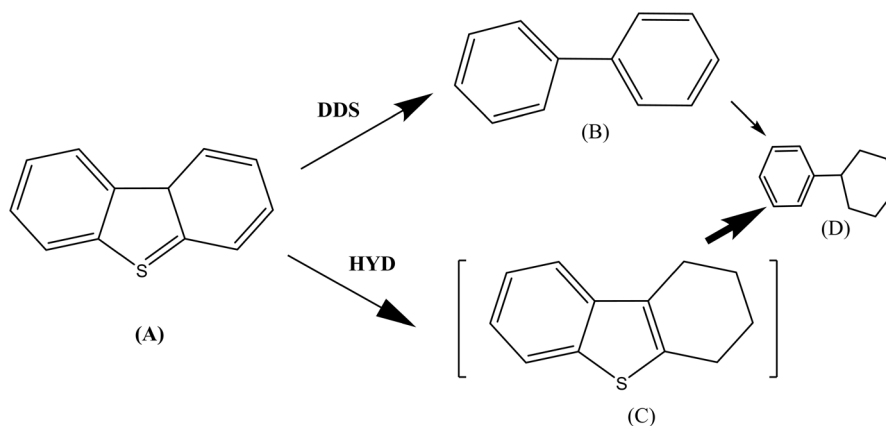


**Figure 2.** Product distributions during the HDS of DBT in the presence of H<sub>2</sub>S.

### 3.1. Kinetics

Several assumptions and simplifications were involved in the kinetics calculations. Firstly, the HDS of DBT was assumed to proceed primarily by DDS and HYD, as in **Scheme 1**.



**Scheme 1.** Intermediate products formed during the HDS reaction of DBT.

In addition, CB was assumed to result mainly from partially-hydrogenated DBT, and so the formation of this product will be promoted by  $\text{H}_2\text{S}$ , in agreement with prior reports [5] [6]. The effect of the  $\text{H}_2$  pressure on the reaction rate was neglected because  $\text{H}_2$  was added in excess and so could be included in the intrinsic rate constant. Two active sites were considered, one for HYD and the other for DDS, according to the equations (all symbols and parameters are identified either in the notation section or in the text):



and

$$A_i = \sigma_D + \pi_H + \pi_H^* + A^*. \quad (3)$$

In this case, the concentration of hydrogenation sites ( $\pi_H$ ) will be affected by the presence of  $\text{H}_2\text{S}$  while the concentration of  $\sigma_D$  sites remains almost unaffected. Two scenarios were considered, consisting of the HDS reaction of DBT with and without  $\text{H}_2\text{S}$ .

### 3.2. Kinetic Model for HDS with a Negligible $\text{H}_2\text{S}$ Concentration

Some prior studies have shown that the HDS of DBT is a pseudo-zero-order reaction [14] [15], while others have determined that this is a pseudo-first-order reaction [7] [12] [16] [17] [18]. As discussed below, the results of the present study agree with the latter behavior and so the analysis in this paper is predicated on pseudo-first-order kinetics. Based on mass balances of the reaction components, rate equations were adapted to quantitatively describe the product distributions. These equations (details of which have been previously published [19]) are:

$$C_D = C_{D_0} \cdot \exp^{-k_0 \cdot t} \quad (4)$$

$$C_B = \frac{C_{A_0} \cdot k_1}{k_3 + k_0} \left[ \exp^{-k_0 \cdot t} - \exp^{-k_3 \cdot t} \right] \quad (5)$$

and

$$C_C = \frac{C_{A_0} \cdot k_2}{k_4 + k_0} \left[ \exp^{-k_0 \cdot t} - \exp^{-k_4 \cdot t} \right] \quad (6)$$

The reaction rate in the absence of H<sub>2</sub>S was well represented by the pseudo-first order relationship in Equation (4), and a plot of the data is presented in **Figure 3**. Here the fit of the experimental points to this equation is confirmed by the high regression factor. Equations (5) and (6) were used to fit the experimental results for the reaction intermediates, which required the iteration estimation of only two variables ( $k_1$  and  $k_2$ ). Each data fitting was performed using the Mathcad software package and employing non-linear methods via sequential iterations until convergence. **Figure 4** plots the concentrations of the intermediate species against reaction time and also shows the fits obtained using Equations (5) and (6), which confirm the validity of the model. Fitting the experimental data with the model allowed the rate constants to be determined, which in turn enabled an estimation of the contribution of intermediates B and C to

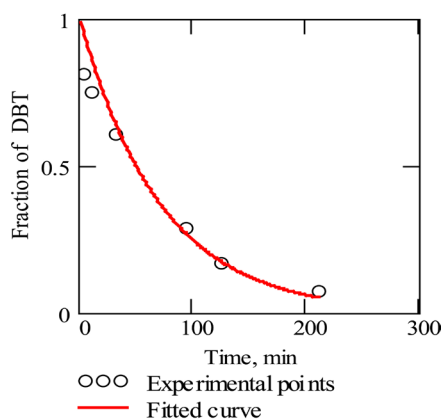


**Figure 3.** Pseudo-first order plots of data acquired during the DBT of HDS in the absence of H<sub>2</sub>S at 340°C and 3 MPa H<sub>2</sub>.

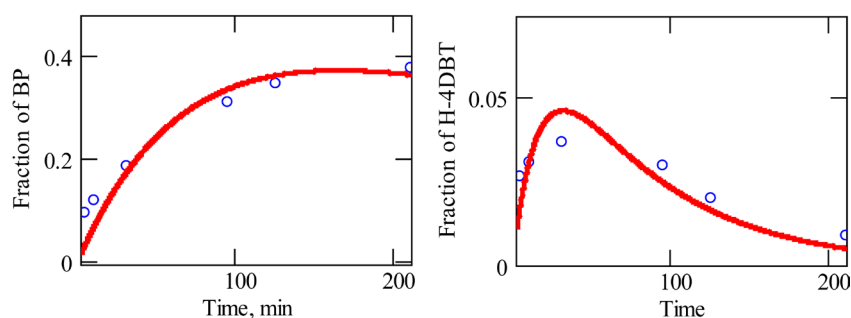


**Figure 4.** Experimental data and fittings for the generation of BP and H4-DBT during the HDS of DBT in the absence of H<sub>2</sub>S.

the yield of D during the HDS reaction. The fractions of B or C transformed to D at a given time  $t$  were estimated from the equations:

$$C_{B \rightarrow D} = \frac{C_{A_0} \cdot k_1}{k_3 + k_0} \left[ \exp^{-k_3 t} \right] \quad (7)$$

and

$$C_{C \rightarrow D} = \frac{C_{A_0} \cdot k_2}{k_{43} + k_0} \left[ \exp^{-k_4 t} \right] \quad (8)$$

The apparent kinetic parameters determined in this manner are provided in **Table 1**. The model used in this work was based on a version of the Langmuir-Hinshelwood mechanism, and so the rate equations for the HYD and DDS reactions were:

$$R_H = k_\pi \cdot \theta_\pi \quad (9)$$

and

$$R_D = k_\sigma \cdot \theta_\sigma \quad (10)$$

By substitution, it is possible to obtain the equations:

$$R_H = \frac{k_\pi \cdot K_\pi \cdot C_D}{1 + K_\pi \cdot C_D} \quad (11)$$

$$R_D = \frac{k_\sigma \cdot K_\sigma \cdot C_D}{1 + K_\sigma \cdot C_D} \quad (12)$$

and

$$R_i = R_H + R_D \quad (13)$$

Once the individual apparent rate constants were found, the equilibrium adsorption constants could be compared. The experimental data were fit according to Equations (11)-(13), as shown in **Figure 5**. Using the apparent rate constants for the parallel reactions determined from the previous calculations, the adsorption equilibrium constants for the substrate on the  $\sigma$  and  $\pi$  sites were predicted and the values are provided in **Table 2**.

### 3.3. Kinetic Model for HDS in the Presence of H<sub>2</sub>S, Promotion Model

Data regarding the product distributions are the primary means of validating

**Table 1.** Kinetic parameters for the HDS of DBT at various H<sub>2</sub>S concentrations.

Reaction condition, (No. of H <sub>2</sub> S moles)	$k_1^*$	$k_2^*$	$k_3^*$	$k_4^*$
No H <sub>2</sub> S	$11.5 \times 10^{-4}$	$11.8 \times 10^{-4}$	$3.2 \times 10^{-4}$	$98.3 \times 10^{-4}$
$\leq 5 \times 10^{-4}$	$5.0 \times 10^{-4}$	$75.0 \times 10^{-4}$		
$17 \times 10^{-4}$	$5.1 \times 10^{-4}$	$75.1 \times 10^{-4}$	$15.2 \times 10^{-4}$	$240.3 \times 10^{-4}$
$23 \times 10^{-4}$	$4.8 \times 10^{-4}$	$75.0 \times 10^{-4}$	$18 \times 10^{-4}$	$236 \times 10^{-4}$
$50 \times 10^{-4}$	$4.5 \times 10^{-4}$	$75.5 \times 10^{-4}$	$17 \times 10^{-4}$	$233 \times 10^{-4}$

\*Individual apparent rate constants, with an uncertainty of approximately 3% - 5%.

any kinetic model, and typical reversible behavior was observed in the present case both with and without H<sub>2</sub>S. This was ascertained by experimental trials during which the reaction was performed using varying concentrations of H<sub>2</sub>S. Under these conditions, the promotional effect of the H<sub>2</sub>S was determined to involve a physical reversible process and was associated with the nature of the catalyst. In the existing of H<sub>2</sub>S, the hydrogenation reaction products were predominant, as can be seen by comparing **Figure 4** and **Figure 6**, and so the activity of this route was obviously increased. The effect of H<sub>2</sub>S can be discussed in terms of its concentration in the reaction feedstock. Because the reaction is carried out in a batch system, a classical treatment of the autocatalytic-like kinetics leads to the equations:

$$R_t = -k_{ts} \cdot C_D \cdot C_S \quad (14)$$

and

$$R_t = -k_{ts} \cdot C_D \cdot (C_{D^0} - C_D) \quad (15)$$

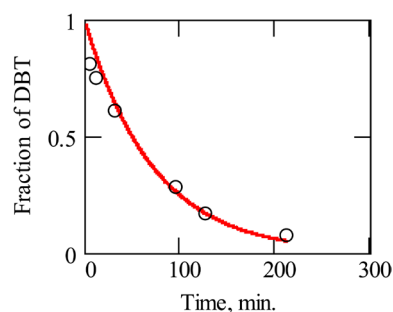


**Figure 5.** Experimental data acquired during the HDS of DBT in the absence of H<sub>2</sub>S and fittings based on the Langmuir-Hinshelwood relationship in Equation (13).

**Table 2.** Equilibrium adsorption constants and kinetic coefficients determined from model fittings for data acquired during the HDS of DBT.

$K_\pi$	$\leq 0.01$	$k_t^a$	$23 \times 10^{-4}$
$K_\sigma$	$\leq 0.01$	$k_{ts}^a$	$80 \times 10^{-4}$
$K_{\pi S}$	$\leq 0.01$		

a: s<sup>-1</sup>·gcat<sup>-1</sup>.

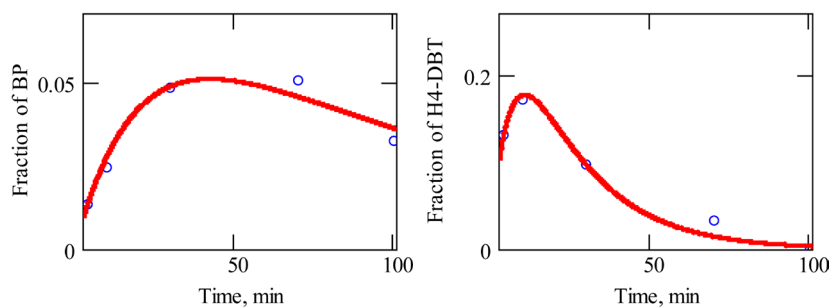


**Figure 6.** Experimental data for the generation of BP and H4-DBT during the HDS of DBT in the presence of  $17 \times 10^{-4}$  moles H<sub>2</sub>S.

Here,  $R_t$  is the total reaction rate and  $k_{ts}$  is the overall rate constant under this conditions. In the present trials, the sum total of the moles of DBT and  $H_2S$  at any given time remained constant, and so we can write:

$$C_t = C_{D^0} + C_{S^0} = C_D + C_S = \text{constant} \quad (16)$$

Equation (15) can be rearranged after integration to:

$$\ln \left[ \frac{C_{D^0} \cdot (C_t - C_D)}{C_D \cdot (C_t - C_{D^0})} \right] = k_{ts} \cdot C_t \cdot t \quad (17)$$

**Figure 7** depicts the experimental data according to this equation, and demonstrates suitable linear regression. Based on the Langmuir-Hinshelwood mechanism, if the  $H_2S$  that is generated *in situ* is retained in the reaction medium, we can write the rate ( $R_{H_2S}$ ) as follows:

$$R_{H_2S} = k_{\pi S} \cdot \theta_{\pi} \cdot (C_S + C_{S^0}) \quad (18)$$

which, after rearrangement and substitution, becomes:

$$R_{H_2S} = \frac{k_{\pi S} \cdot K_{\pi} \cdot C_D \cdot (C_S + C_{S^0})}{1 + K_{\pi} \cdot C_D + K_{\pi S} \cdot (C_S + C_{S^0})} \quad (19)$$

The DDS route is not considered to be affected by the presence of  $H_2S$ , and so we have:

$$R_{D,S} = \frac{k_{\sigma} \cdot K_{\sigma} \cdot C_D}{1 + K_{\sigma} \cdot C_D} \quad (20)$$

This indicates a special case in which the reaction rate exhibits autocatalytic-like behavior. In an autocatalytic process, one of the reaction products is involved in the catalytic mechanism and so should be included in the rate law. During HDS over the present  $MoS_2$  catalyst, the reaction rate was found to be promoted by  $H_2S$ , and thus this species may affect both the potential and the nature of the active catalytic sites. Therefore, the overall rate in the presence of  $H_2S$  that is generated *in situ*,  $R_{ts}$ , can be represented as:

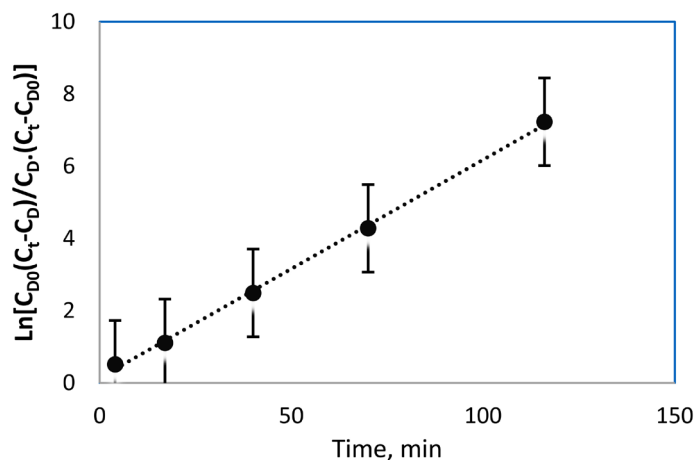


**Figure 7.** A linear plot confirming the autocatalytic nature of the HDS of DBT, based on Equation (17).



$$R_{ts} = R_{H-S} + R_{D-S} \quad (21)$$

where  $R_{ts}$  is the overall reaction rate. The correlation associated with Equation (21) is depicted in **Figure 8** and shows a suitable fit to the experimental data. Based on the constants estimated from both the classical treatment and the data analysis using Equations (19)-(21), the adsorption equilibrium constant associated with  $H_2S$  can be determined, and the results of such calculations are provided in **Table 2**.

### 3.4. Analysis of the Kinetic Data

In model simulations, as the constants utilized in the model remain limited in number then the validity of model to be adopted increased. To minimize the number of constants included in our kinetic model, we first calculated reaction parameters based on the proposed model of Equations (5) and (6), and then estimated the fraction of each intermediate product that participates in the reaction, followed by manipulating the kinetic treatments once more according to the promotion model. From these calculations, the ratio of the DBT adsorption equilibrium constant for  $\pi$  sites to that for  $\sigma$  sites was found to be close to unity. Thus, there was no preferential adsorption of the reactant on either active site when using the present catalyst. It should be noted that the adsorption equilibrium constants were estimated to have this limited value  $K_\sigma$  or  $K_\pi \leq 0.01$  and that the ratio of  $K_\pi/K_\sigma \approx 1$ . Based on prior research regarding HDS reactions and the kinetic parameters estimated in this study, it is possible to analyze the experimental data as follows.

#### 3.4.1. First Stage

When the HDS reaction was performed in the absence of  $H_2S$ , the data could be fitted with a model recently developed by our group in which all the reaction products are included in the rate equations (that is, Equations (4)-(6)). This model was subsequently used to simulate the experimental data shown in **Figure 4** and a reasonable agreement between the experimental values and the simulation can be seen. The estimated values predicted by this model are presented in **Table 1**. If the HDS process proceeds as a pseudo-first-order reaction, then this

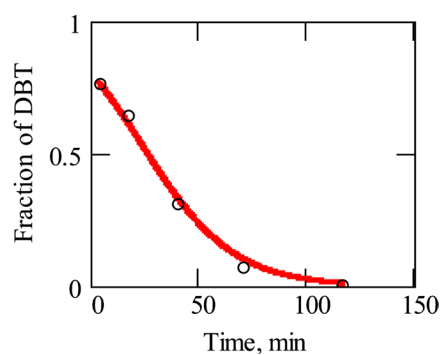


**Figure 8.** Experimental data acquired during the HDS of DBT in the presence of  $H_2S$  with fitting based on Equation (21).

model may be applicable.

### 3.4.2. Second Stage

If the H<sub>2</sub>S generated *in situ* remains in the reaction mixture, a kinetic rate curve corresponding to autocatalytic behavior is obtained, as is evident in **Figure 7** and **Figure 8**. In this case, models based on Equations (17) and (21) were applied to simulate the experimental data for the overall reaction, and these predictions matched the trend exhibited by the experimental values. The equilibrium constants for substrate adsorption on the two active sites and their ratios should certainly be considered primarily on applying this model. In addition, the rate constants for the two parallel routes (*i.e.*, DDS and HYD) should be taken into consideration when fitting data acquired in the presence of H<sub>2</sub>S. For this reason, the estimated HDS kinetic parameters for the reaction in case of absence of H<sub>2</sub>S were utilized to assess the reaction in the presence of H<sub>2</sub>S. Including such limits may help improve the simulation results. The results clearly showed that there was little change in the DBT and H<sub>2</sub>S adsorption equilibrium constants and that the values of these constants remained  $\leq 0.01$ .

### 3.4.3. Third Stage

In presence of an excess of H<sub>2</sub>S, a part of this species modifies the potential active sites while the rest is essentially not involved in the reaction. This scenario is quite similar to that in an actual refinery performing HDS. The catalyst may be involved in the reaction in a manner which is kinetically similar in nature to that found in the first stage section. The model discussed above in relation to the first stage can also be applied to describe this reaction, and the associated kinetic data are listed in **Table 1**. It is interesting to observe that the H<sub>2</sub>S has an effect following the first dose, such that the reaction proceeds as though the H<sub>2</sub>S undergoes self-promotion. Thereafter, with increases in the H<sub>2</sub>S concentration in the feedstock, its primary effect remains almost unchanged and the reaction behaves kinetically as a pseudo-first-order process. This effect can possibly be attributed to the formation of new active sites created by the H<sub>2</sub>S. After an equilibrium is achieved, at which point the H<sub>2</sub>S has modified all possible potential active sites, the reaction proceeds normally through the participation of the two kinds of active sites. Thus, the self-promotion effect induced by H<sub>2</sub>S is basically temporary and is associated with the modification of active sites up to saturation. Another point to note is that an excess of H<sub>2</sub>S induces neither further promotion nor inhibition of the catalytic activity, **Figure 9**. These results emphasize that H<sub>2</sub>S acts as a promoter possibly by increasing the efficiency of active sites, by increasing the number of sites, or by both mechanisms.

## 3.5. Inhibition and Promotion

At present, there is a lack of full information regarding the effect of compounds such as H<sub>2</sub>S and organic nitrogen compounds on catalytic behavior during HDS over unsupported bulk MoS<sub>2</sub> catalysts. The presence of H<sub>2</sub>S evidently inhibits the

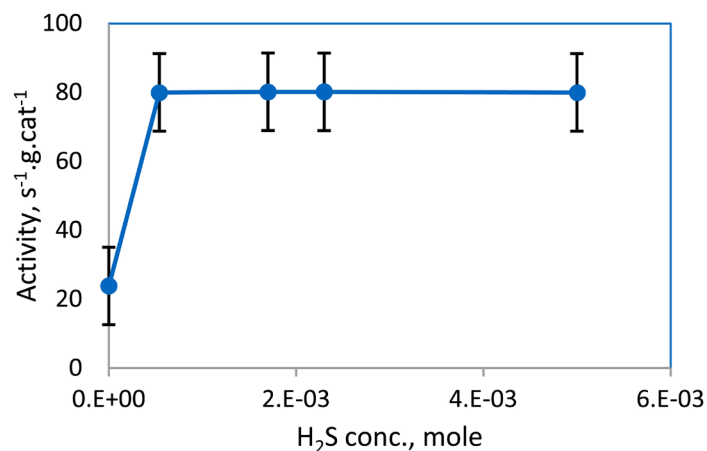


**Figure 9.** Catalytic activity versus the H<sub>2</sub>S amount in the feedstock.

DDS reaction of polyaromatic refractory sulfur containing compounds but has little impact on the HYD pathway. This detrimental effect on activity is apparent when employing conventional catalysts. As an example, an inhibition effect was reported in reactions using conventional CoMo/Al<sub>2</sub>O<sub>3</sub> catalysts, and was also reported to be reversible [7]. The present results concerning the MoS<sub>2</sub> catalyst show a remarkable enhancement of the HYD route upon the addition of H<sub>2</sub>S. Two kinetic models are proposed: one in the absence of H<sub>2</sub>S and the other with H<sub>2</sub>S in the reaction medium at moderate levels. H<sub>2</sub> appears to be essential to the HDS process and may play a specific role in modifying the potential active sites that become two independent types: for the HYD and DDS reactions. The experimental results in the absence of H<sub>2</sub>S can be reasonably described by the model based on Equations (4)-(6). In contrast, in the presence of H<sub>2</sub>S, the occurrence of HYD is promoted and the overall catalytic activity is enhanced. This improvement in the activity is obviously due to the increased rate of the HYD reaction. The effect of H<sub>2</sub>S on kinetics leads to the hypothesis that H<sub>2</sub>S interacts chemically with the catalyst by creating new highly active HYD sites. The good agreement of the experimental results with the non-linear numerical fitting supports this hypothesis.

Thus, H<sub>2</sub>S is believed to act as a reagent to create a fixed number of potential HYD active sites. These sites can be modified either by H<sub>2</sub> or H<sub>2</sub>S. While H<sub>2</sub> modification of the active sites leads to two distinct types of sites for the two routes, H<sub>2</sub>S modifies the active sites to selectively promote the HYD reaction. The efficiency of the HYD active sites created by H<sub>2</sub>S is likely much more pronounced than those generated by H<sub>2</sub>. The present results and the fitting models also suggest the potential for mutual interconversion of the newly created active sites. Egorova *et al.* [5] reported that H<sub>2</sub>S has a positive effect on the cleavage of C-N bonds. It is unclear if this effect is due to the sulfidation state of the catalyst or to the participation of H<sub>2</sub>S in the reaction mechanism, although the authors suggest the latter. The present study supports this hypothesis too. This unique behavior of H<sub>2</sub>S in conjunction with this particular bulk MoS<sub>2</sub> catalyst during

HDS is opposite to the behavior reported with conventional catalysts. These results confirm the importance of the structure of the MoS<sub>2</sub> species, and suggest that not all such species will show similar effects together with H<sub>2</sub>S.

#### 4. Conclusion

Kinetic models based on the assumption of two distinct active sites for DDS and HYD during the HDS of DBT over a MoS<sub>2</sub> catalyst were constructed and exhibited good agreement with experimental results. According to these models, H<sub>2</sub>S promotes HYD via its chemical involvement in the reaction mechanism, while H<sub>2</sub> produces two distinct active sites: one for HYD and the other for DDS. The presence of H<sub>2</sub>S might lead to the formation of new and highly effective HYD active sites. Because of the fixed number of active sites that can be activated either by H<sub>2</sub> or H<sub>2</sub>S, it is important to consider the quantity of newly created sites as a ratio of the total number of sites when assessing selectivity. Thus, as HYD active sites ( $\pi^*$ ) are increased in number, the quantity of DDS active sites ( $\sigma$ ) decreases. Overall, this study suggests that two reaction mechanisms are possible, depending on whether or not H<sub>2</sub>S is present in the reaction medium. It can be inferred that the HDS reaction can be promoted by including an optimal H<sub>2</sub>S concentration in the reaction feedstock so as to create more active sites.

#### Acknowledgements

This work was supported by Kyushu University, Japan, and Mansoura University, Egypt.

#### Conflicts of Interest

The authors declare no conflicts of interest regarding the publication of this paper.

#### References

- [1] Whitehurst, D.D., Isoda, T. and Mochida, I. (1998) Present State of the Art and Future Challenges in the Hydrodesulfurization of Polyaromatic Sulfur Compounds. *Advances in Catalysis*, **42**, 345-471. [https://doi.org/10.1016/S0360-0564\(08\)60631-8](https://doi.org/10.1016/S0360-0564(08)60631-8)
- [2] Zdrzil, M. (1991) Effect of Reaction Conditions, Transition Metal and Synergism on Selectivity in Hydrotreatment. *Bulletin des Sociétés Chimiques Belges*, **100**, 769-780. <https://doi.org/10.1002/bscb.19911001101>
- [3] Girgis, M. and Gates, B. (1991) Reactivities, Reaction Networks and Kinetics in High Pressure Catalytic Hydroprocessing. *Industrial & Engineering Chemistry Research*, **30**, 2021-2058. <https://doi.org/10.1021/ie00057a001>
- [4] Pille, R.C., Yu, C. and Froment, G.F. (1994) Kinetic Study of the Hydrogen Sulfide Effect in the Conversion of Thiophene on Supported CoMo Catalysts. *Journal of Molecular Catalysis*, **94**, 369-387. [https://doi.org/10.1016/0304-5102\(94\)00152-9](https://doi.org/10.1016/0304-5102(94)00152-9)
- [5] Egorova, M. and Prins, R. (2004) Mutual Influence of the HDS of Dibenzothiophene and HDN of 2-Methylpyridine. *Journal of Catalysis*, **221**, 11-19. [https://doi.org/10.1016/S0021-9517\(03\)00264-1](https://doi.org/10.1016/S0021-9517(03)00264-1)
- [6] Robinson, W.R.A.M., van Veen, J.A.R., de Beer, V.H.J. and van Santen, R.A. (1999)

- Development of Deep Hydrodesulfurization Catalysts I. CoMo and NiMo Catalysts Tested with Substituted Dibenzothiophene. *Fuel Processing Technology*, **61**, 89-101. [https://doi.org/10.1016/S0378-3820\(99\)00033-8](https://doi.org/10.1016/S0378-3820(99)00033-8)
- [7] Sie, S.T. (1999) Reaction Order and Role of Hydrogen Sulfide in Deep Hydrodesulfurization of Gas Oils: Consequences for Industrial Reactor Configuration. *Fuel Processing Technology*, **61**, 149-171. [https://doi.org/10.1016/S0378-3820\(99\)00036-3](https://doi.org/10.1016/S0378-3820(99)00036-3)
- [8] Kabe, T., Aoyama, Y., Wang, D., Ishihara, A., Qian, W., Hosoya, M. and Zhang, Q. (2001) Effects of H<sub>2</sub>S on Hydrodesulfurization of Dibenzothiophene and 4,6-Dimethyldibenzothiophene on Alumina-Supported NiMo and NiW Catalysts. *Applied Catalysis A: General*, **209**, 237-247. [https://doi.org/10.1016/S0926-860X\(00\)00770-5](https://doi.org/10.1016/S0926-860X(00)00770-5)
- [9] Liu, B., Chai, Y., Li, Y., Wang, A., Liu, Y. and Liu, C. (2014) Kinetic Investigation of the Effect of H<sub>2</sub>S in the Hydrodesulfurization of FCC Gasoline. *Fuel*, **123**, 43-51. <https://doi.org/10.1016/j.fuel.2014.01.055>
- [10] Rana, M.S., Ancheyta, J., Rayo, P. and Maity, S.K. (2007) Heavy Oil Hydroprocessing over Supported NiMo Sulfided Catalyst: An Inhibition Effect by Added H<sub>2</sub>S. *Fuel*, **86**, 1263-1269. <https://doi.org/10.1016/j.fuel.2006.08.002>
- [11] Farag, H. and Sakanishi, K. (2004) Investigation of 4,6-Dimethyldibenzothiophene Hydrodesulfurization over a Highly Active Bulk MoS<sub>2</sub> Catalyst. *Journal of Catalysis*, **225**, 531-535. <https://doi.org/10.1016/j.jcat.2004.05.001>
- [12] Farag, H., El-Hendawy, A.-N.A., Sakanishi, K., Kishida, M. and Mochida, I. (2009) Catalytic Activity of Synthesized Nanosized Molybdenum Disulfide for the Hydrodesulfurization of Dibenzothiophene: Effect of H<sub>2</sub>S Partial Pressure. *Applied Catalysis B: Environmental*, **91**, 189-197. <https://doi.org/10.1016/j.apcatb.2009.05.023>
- [13] Vogelaar, B.M., Kagami, N., Van Langeveld, A.D., Eijssbouts, S. and Moulijn, J.A. (2003) Active Sites and Activity in HDS Catalysis: The Effect of H<sub>2</sub> and H<sub>2</sub>S Partial Pressure. *American Chemical Society Division of Fuel Chemistry*, **48**, 548-549.
- [14] Daage, M. and Chianelli, R.R. (1992) Structure-Function Relations in Molybdenum Sulfide Catalysts: The "Rim-Edge" Model. *Journal of Catalysis*, **149**, 414-427. <https://doi.org/10.1006/jcat.1994.1308>
- [15] Sollner, J., Gonzalez, D.F., Leal, J.H., Eubanks, T.M. and Parsons, J.G. (2017) HDS of Dibenzothiophene with CoMoS<sub>2</sub> Synthesized Using Elemental Sulfur. *Inorganica Chimica Acta*, **466**, 212-218. <https://doi.org/10.1016/j.ica.2017.06.028>
- [16] Kim, J.H., Ma, X., Song, C., Lee, Y.-K. and Oyama, S.T. (2005) Kinetics of Two Pathways for 4,6-Dimethyldibenzothiophene Hydrodesulfurization over NiMo, CoMo Sulfide, and Nickel Phosphide Catalysts. *Energy and Fuels*, **19**, 353-364. <https://doi.org/10.1021/ef049804g>
- [17] Valencia, D. and Klimova, T. (2012) Kinetic Study of NiMo/SBA-15 Catalysts Prepared with Citric Acid in Hydrodesulfurization of Dibenzothiophene. *Catalysis Communications*, **21**, 77-81. <https://doi.org/10.1016/j.catcom.2012.02.003>
- [18] Méndez, F.J., Franco-López, O.E., Bokhimi, X., Solís-Casados, D.A., Escobar-Alarcón, L. and Klimova, T.E. (2017) Dibenzothiophene Hydrodesulfurization with NiMo and CoMo Catalysts Supported on Niobium-Modified MCM-41. *Applied Catalysis B: Environmental*, **219**, 479-491. <https://doi.org/10.1016/j.apcatb.2017.07.079>
- [19] Farag, H. (2006) Kinetic Analysis of the Hydrodesulfurization of Dibenzothiophene: Approach Solution to the Reaction Network. *Energy and Fuels*, **20**, 1815-1821. <https://doi.org/10.1021/ef060225g>

**Notation**

$\pi_H^*$	Active hydrogenation sites generated by H <sub>2</sub> S
$\pi_H$	Active hydrogenation sites generated by H <sub>2</sub>
$\sigma_D$	Active direct desulfurization sites
$A^*$	Potential active sites
$k_1$	Rate constant for the hydrogenation of DBT
$k_2$	Rate constant for DDS
$k_3$	Rate constant for BP hydrogenation
$k_4$	Rate constant for the hydrogenation of DBT
$k^*$	Sum of $k_1$ and $k_2$
$K_\pi$	Equilibrium constant for the adsorption of DBT on $\pi$ sites
$K_\sigma$	Equilibrium constant for the adsorption of DBT on sigma sites
$K_{\pi S}$	Equilibrium constant for the adsorption of H <sub>2</sub> S on $\pi$ sites
$k_\pi$	Intrinsic rate constant for hydrogenation
$k_\sigma$	Intrinsic rate constant for DDS
$k_{\pi S}$	Intrinsic rate constant for hydrogenation in the presence of H <sub>2</sub> S
$k_t$	Overall rate constant in the absence of H <sub>2</sub> S
$k_{ts}$	Overall rate constant in the presence of H <sub>2</sub> S
$C_D$	Concentration of DBT at time $t$
$C_S$	Concentration of H <sub>2</sub> S
$C_H$	Concentration of HDBT
$C_B$	Concentration of BP
$C_{D^0}$	Initial concentration of DBT
$C_{S^0}$	Initial concentration of H <sub>2</sub> S
$R_{H-S}$	Rate based on Langmuir-Hinshelwood mechanism